Printable Chipless Tag and Dual-CP Reader for Internet of Things

Guoqing Dong, Yizhu Shen, Hongfu Meng, Na Chen, Wenbin Dou, and Sanming Hu

State Key Laboratory of Millimeter Waves
Southeast University, Nanjing, 210096, China
sanming.hu@seu.edu.cn

Abstract ─ This paper proposes a printable chipless tag that encodes more bits than a conventional tag, and also a dual circularly polarized (CP) reader that achieves high isolation with insensitive orientation. To demonstrate this concept, a radio-frequency identification (RFID) tag of 13mm×13mm is designed to encode 5 bits covering 6 - 9 GHz. This tag is investigated and measured with dual-CP backscattering characteristics for the first time. The versatile dual-CP reader, along with this tag which is feasible to print on other flexible substrate including papers, clothes and plastics, are promising to benefit the Internet of Things (IoT).

Index Terms ─ Chipless tag, dual circular polarization, Internet of Things (IoT), Radar Cross Section (RCS), Radio-Frequency Identification (RFID).

I. INTRODUCTION

Different from the widely employed barcode technology, radio frequency identification (RFID) adopts electromagnetic wave to identify targets [1]. RFID has been widely applied to many scenarios including transportation tolls, animal ID, and anti-thief systems, etc. [2]. RFID system usually consists of three parts: tags that carry binary information, readers that extract the encoded data, and a general platform connected with the Internet. Printable RFID tags, which features long reading range, non-line-of-sight (NLOS) reading, and automated identification and tracking, have the potential to supplement the existing barcode technology [3]. The popularity of RFID is mainly dependent on the cost of the tag, especially the cost of silicon chip in a tag. Therefore, chipless RFID tag without expensive chips has become the industry trend and attracts intensive research interest for low-cost, and massive item identification and tracking.

A chipless tag contains neither IC chips nor battery. Therefore, it's very challenging to encode as many data bits as chipped tag. To solve this problems, four encoding methods based on time, frequency, phase, and image are investigated. Among these, the frequency-domain-based approach are demonstrated with the highest data storage capabilities [4]. Using this method, chipless tags are designed with resonators to encode data into predetermined spectrum, and each data bit is associated with the presence or absence of a resonant peak [3]. Based on this principle, many different tags are proposed in [5-7]. However, to date, there still exist two issues. Firstly, the reading accuracy is seriously dependent on the position, orientation, and polarization of chipless tags. Secondly, the RFID system generally requires high isolation between transmitting (Tx) and receiving (Rx) antennas in reader, which causes the complexity and high cost of reader [8].

To alleviate the above issues, this paper demonstrates a novel dual circularly-polarized (dual-CP) RFID system as proposed in [9]. This dual-CP RFID system includes a compact linearly-polarized tag and a pair of reader antennas operating with left-handed circular polarization (LHCP) and right-handed circular polarization (RHCP) respectively. This system features high isolation between Tx and Rx, which not only alleviates the complexity of the following front-end circuits for signal extraction, but also makes the tags orientation insensitive. Additionally, by introducing a dummy structure, one more bit is achieved in the upper ultra-wideband (UWB) frequency range of 6-9 GHz. This paper is organized as follows. Section II introduces the design and analysis of chipless tag and presents the RCS measurements of chipless RFID tags. Section III shows the tag's performance as well as the measurement of RCS for the tag. And last part, Section IV is the conclusion.

II. TAG DESIGN AND MEASUREMENT PRINCIPLE

A. Tag design principle

The proposed dual-CP RFID system is shown in Fig. 1. It consists of two antennas with crossed polarization, i.e., LHCP and RHCP, for transmitting and receiving respectively. Therefore, the isolation between Tx and Rx of the RFID readers is significantly increased. Moreover, this dual-CP configuration enables the proposed RFID system to detect tags with arbitrary orientation. The operation frequency is set as 6-9 GHz which is assigned by the Ministry of Industry and Information Technology of the People's Republic of China for ultra-wideband

Submitted On: September 30, 2017
Accepted On: April 21, 2018

applications [10].

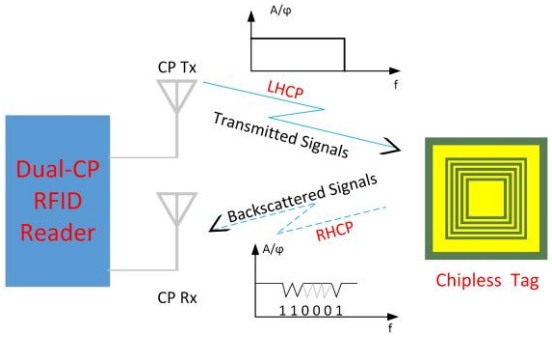

Fig. 1. The proposed RFID system with a dual-CP reader and a chipless tag.

Coplanar square slots with nested concentration structure are used for the tag design. The structure features narrower bandwidth than other resonators such as circular rings. In addition, square slots are more reluctant to the printing errors than other shapes [4], especially when the operating frequency is much higher than the ultra-high-frequency (UHF), the printing accuracy should be the first priority.

For the square-slots, the length dimension of each half-loop should be a multiple of the half-wavelength for resonance to occur, which means each half-loop is acting as a dipole element and the length dimension of the whole loop needs, therefore, to be a multiple of one full wavelength. However, to avoid weak resonances of re-radiated energy in hemisphere of a single element, the length of the loop must be one wavelength instead of a multiple-wavelength [11].

Square slots resonators with different lengths are formulated to generate different signature to represent one bit. Actually, each square slot works as a λ resonator, which means its circumference is equal to one phase wavelength (λ_g) as expressed in Equation (1):

$$\lambda_g = 2(L_i + L_i - 2W_i), \quad (1)$$

and

$$L_i = L_{i-1} - W_{i-1} - G_{i-1}, \quad (2)$$

where L_i is the side length of corresponding slot resonator, W_i is the width of corresponding square slot, G_i is the gap between them. However, the loop width (W) and substrate thickness (h) are also considered for calculating the guided wavelength (λ_g) of the square loop resonator. These empirical equations are derived from least square curve fitting techniques [12] which is quite complex to construct the design.

For simplicity, we can derive the resonant frequency as:

$$f_i = \frac{c}{2(L_i+L_i-2W_i)}\sqrt{\frac{2}{\varepsilon_r+1}}, \quad (3)$$

where c is the speed of light in free space, L_i is the side length of corresponding square slot resonator, and ε_r is the relative permittivity of the substrate.

Therefore, if N square slots of different lengths are placed concentrically, it will generate signatures with N different frequencies. Meanwhile, the harmonics have no effect on the tag's performance: the second harmonics of the resonance are absent in the backscattered signal, while the third harmonics are out of the operation band (6-9 GHz) and small enough to be neglected.

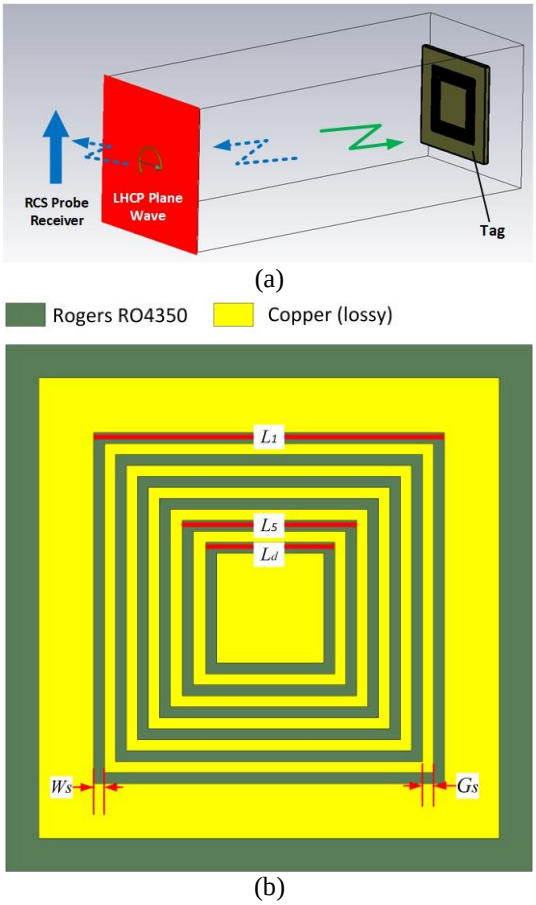

Fig. 2. The proposed chipless tag: (a) design schematic and (b) tag parameters.

As shown in Fig. 2 (a), the tag is excited by LHCP plane wave and the frequency-encoded backscattered signal from the tag is received by an RCS probe placed at 50 mm away. Open (add space) boundary condition is used during the simulation.

The layout of the proposed 5-bit tag is shown in Fig. 2 (b) with design parameters, where L_1 and L_5 are the side lengths of the outermost and innermost square slot resonator respectively, L_d is the side length of the dummy structure. The square slots are with the same width of W_s and gap of G_s between each other. They are calculated using Equation (1), with detailed parameters of L_1 = 8.4mm, L_5 = 6.0mm, L_d = 5.4mm, and W_s = G_s = 0.15mm. The substrate is Rogers RO4350, with dielectric constant of

3.48, and a thickness of 0.76 mm.

The resonators are numbered according to their lengths: resonator 1 is the longest resonator and generates the lowest frequency, which is denoted as most significant bit (MSB); while resonator 5 with highest frequency is denoted as least significant bit (LSB).

When the incident plane wave excites this square slot tag as shown in Fig. 2 (a), a frequency-selective behavior with deep notches appear at the resonant frequencies in the backscattered signal. However, because of the same width and gap of these square loops, the resonant quality factor will drop at higher resonant frequency points, with increased resonant bandwidth. Therefore, a dummy structure is innovatively proposed and located at the inner part of resonator 5. This introduced dummy structure will bring one more bit.

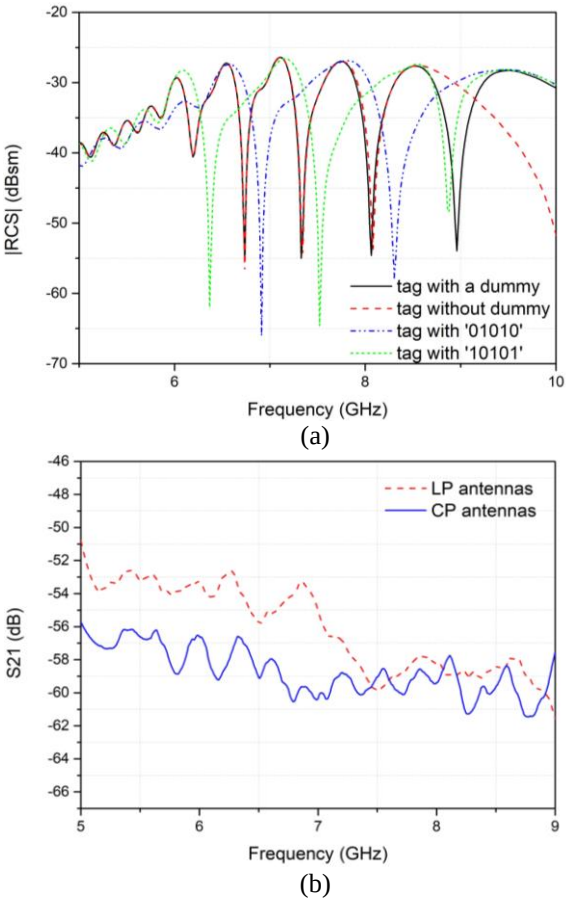

Fig. 3. (a) RCS performance of the four different tags, and (b) the isolation between two horn antennas in the two different RFID systems (@200mm distance).

As shown in Fig. 3 (a), if employing the conventional structure with five square resonators, the six resonant frequency is out of the frequency range of 6-9 GHz, and its Q-factor is too low to be detected as a resonance. Thus, a dummy is innovatively added at the inner of the shortest square resonator to narrow the bandwidth of the highest resonance.

The isolation between two CP and LP horn antennas was demonstrated respectively. The two antennas were placed straightly at 200mm distance. As depicted in Fig. 3 (b), at comparatively lower frequency (5-7 GHz), the isolation between the two LP horn antennas is quite lower compared with CP ones. Since the RCS response of single tag is weak, one tag reading range is quite limited in LP RFID system. As a result, our dual-CP RFID system is free from poor isolation performance, and thus has a farther reading range of tags than conventional LP RFID system.

B. RCS measurement methods

RCS measurement is usually based on the far-field measurement of the backscattered power from the target, namely the tag in this circumstance. The value can be obtained by using vector network analyzer (VNA). As illustrated in Fig. 4, there are two possible measurement configurations: the bi-static bench with two antennas and the mono-static bench with only one antenna. The backscattered power transfer is characterized by the transmission coefficient in bi-static bench and the reflection coefficient in mono-static bench [13].

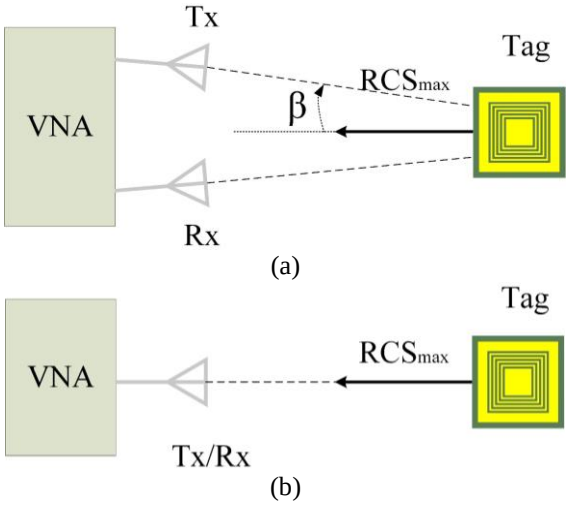

Fig. 4. Configuration of two possible measurement benches: (a) bi-static (measurement of the S_{21} parameter), and (b) mono-static (measurement of the S_{11} parameter).

If the target responds in cross-polarization, a dual-CP antenna can be used as probe, avoiding the environmental contribution such as in [14] and overcoming the incident angle issue [13]. In this configuration, the isolation between the two ports of this antenna will be a critical parameter of the testing accuracy. Hence, we use bi-static RCS measurement configuration. RFID systems can be treated as radar systems because the backward communication link (from tags to the reader) is purely

scattering.

Basically, the RCS can be determined by measuring the backscattered power and using the radar equation in which transmitting power and receiving power have relation formulating in Equation (4) [15]:

$$P_r = \frac{P_t G_t G_r \lambda^2 \sigma}{(4\pi)^3 R^4}, \quad (4)$$

where P_t is transmitting power, P_r is receiving power, G_t, G_r are respectively gain of Tx and Rx, λ is transmitting wave length, R is distance between antenna and tag, σ is the RCS of the tag. The Tx and Rx transmission coefficient from VNA can be obtained using Equation (5):

$$P_r / P_t = |S_{21}|^2 . \quad (5)$$

As a result, the RCS of the tag is calculated with (2) and (6):

$$\sigma = \frac{(4\pi)^3 R^4 |S_{21}|^2}{G_t G_r \lambda^2}, \quad (6)$$

Another RCS calculation method can be found in [16] that RCS σ_{tag} of tags under test is as a function of the frequency based on the known RCS σ_{ref} of the reference scatter:

$$\sigma_{tag} = \left[\frac{S_{21}^{tag} - S_{21}^{background}}{S_{21}^{ref} - S_{21}^{background}} \right]^2 \sigma_{ref}, \quad (7)$$

where $S_{21}^{background}$ is measured S_{21} parameter when nothing is mounted and S_{21}^{ref} is measured S_{21} parameter when the reference scatter is mounted. Normally, a flat metal plate or a metal ball is used as the reference target.

When a perfectly-conducting square flat plate, of side length a, is considered, its RCS can be expressed as [17]:

$$\sigma = \frac{4\pi a^4}{\lambda^2}, \quad (8)$$

or in general, for a plate of area A,

$$\sigma = \frac{4\pi A^2}{\lambda^2}, \quad (9)$$

the RCS has units of m^2 and is often expressed in decibels relative to square meter (dBsm):

$$\sigma(\text{dBsm}) = 10\log_{10}[\sigma(m^2)]. \quad (10)$$

III. RESULTS

Tag measurement was setup in the bi-static form as shown in Fig. 5 (a). The tag doesn't have ground plane; therefore, when the tag was illuminated with LHCP wave, EM waves can be received at both sides of the tag. Figure 6 (a) shows the backscattered signal. The RHCP component is dominant and in the front direction, i.e., the ratio of RHCP/LHCP is much higher than 0 dB. On the contrary, as shown in Fig. 6 (b), LHCP is dominant from the back side. Therefore, it is feasible to use dual-CP antennas to detect these tags.

To improve the RCS response of proposed chipless tags, we fabricated the tag in the form of 4×4 arrays as depicted in Fig. 5 (b). From Equation (4), we can derive the relation between the two RCS response of array and unit:

$$\sigma_{array}(dB) - \sigma_{unit}(dB) = 10log_{10}(16)=12.04. \quad (11)$$

The RCS response in Fig. 7 shows that, when the incident plane wave has limited angle with the tag, there is almost no obvious orientation mismatch, i.e., the proposed dual-CP system can read tags with different orientation.

As Fig. 4 depicts, when we employ the bi-static measurement of S-parameter or RCS response, deviation is unavoidable as the angle deviation increases. Given in Fig. 8, keeping the resonant frequency within acceptable range, the angle between the two antennas can be up to 45 degrees, which is enough for real applications.

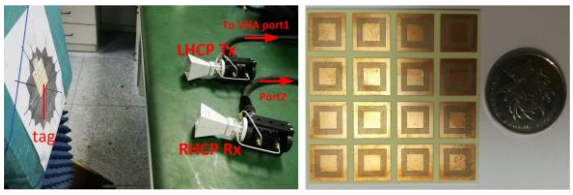

(a) (b)

Fig. 5. (a) Tag measurement setup using two CP horn antennas, and (b) prototype of proposed tag with '11111' (4x4 array).

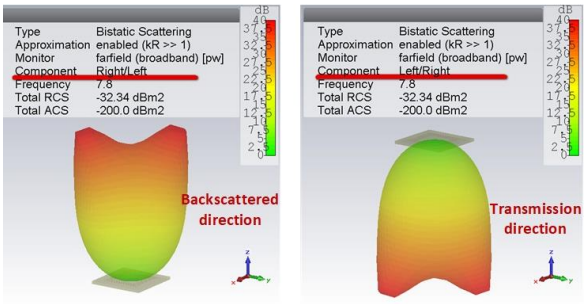

(a) (b)

Fig. 6. Dual-CP backscattering characteristics of the proposed tag: (a) RHCP/LHCP ratio at the front side, and (b) LHCP/RHCP ratio at the back side.

IV. CONCLUSION

A dual-CP RFID system with high isolation and printable chipless nested square slots tag with higher density is proposed and demonstrated. By introducing a dummy, we achieved 1 more bit covering 6−9 GHz. This tag can be directly printed on versatile substrate. In addition, the dual-CP system is orientation insensitive and have 45 degrees tolerance between Tx and Rx. The measured results show that, the proposed dual-CP

system with chipless tag is promising for low-cost IoT applications.

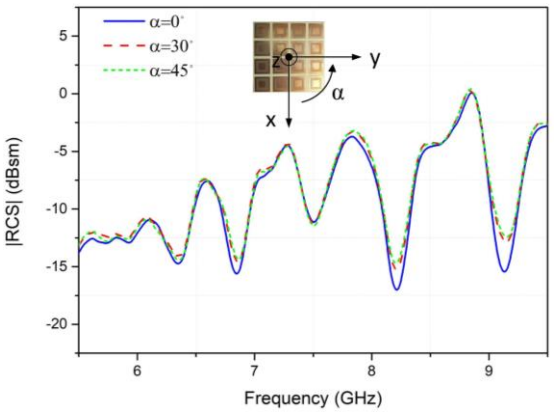

Fig. 7. Measured RCS results for tag with dummy structure, for three angles of incident wave (tag lying on the xoy plane).

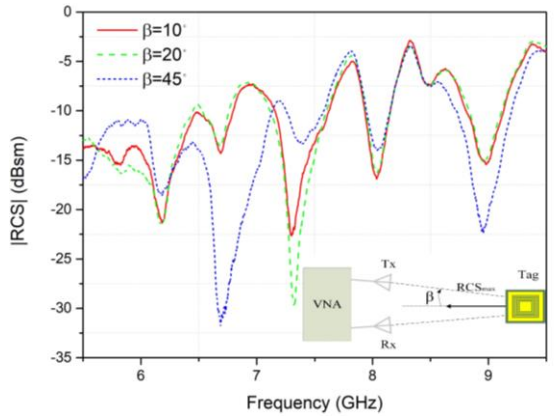

Fig. 8. Angle deviation tolerance of tag with dummy structure for example.

ACKNOWLEDGMENT

This work was supported in part by the National Natural Science Foundation of China under Grants 61701111 and 61701112, and in part by the Open Project Program of the State Key Laboratory of Millimeter Waves under Grants Z201701 and Z201702.

REFERENCES

[1] H. Stockman, "Communication by means of reflected power," *Proc. IRE*, pp. 1196-1204, 1948.

[2] K. Finkenzeller, *RFID Handbook: Fundamentals and Applications in Contactless Smart Cards, Radio Frequency Identification and Near-Field Communication*. New York, NY, USA: Wiley, 2010.

[3] S. Preradovic and N. C. Karmakar, "Chipless RFID: Bar code of the future," *IEEE Microw. Mag.*, pp. 87-97, 2010.

[4] M. A. Islam and N. C. Karmakar, "Real-world implementation challenges of a novel dual-polarized compact printable chipless RFID tag," *IEEE Trans. Microw. Theory Techn.*, vol. 63, no. 12, pp. 4581-4591, 2015.

[5] Md. Aminul Islam, "Compact Printable Chipless RFID Systems," Ph.D. Thesis, Monash University, Melbourne, Australia, 2014.

[6] R. Rezaiesarlak and M. Manteghi, *Chipless RFID, Design Procedure and Detection Techniques.* New York, NY, USA: Springer, 2015.

[7] S. Preradovic, *et al.*, "Multiresonator-based chip item tracking," *IEEE Trans. Microw. Theory Techn.*, vol. 57, pp. 1411-1419, 2009.

[8] T. Björninen, *et al.*, "Circularly polarized tag antenna for UHF RFID," in *26th Annual Review of Progress in Applied Computational Electromagnetics*, Tampere, 2010.

[9] G. Dong, Y. Shen, H. He, J. Virkki, and S. Hu, "Chipless graphene tag and dual-CP reader for Internet of Things," in *2017 International Applied Computational Electromagnetics Society Symposium*, Suzhou, 2017.

[10] Ministry of Industry and Information Technology of the People's Republic of China, April 3, 2013. [Online]. Available: http://www.miit.gov.cn/n1146285/n1146352/n3054355/n3057735/n3057748/n3057752/c3653822/content.html

[11] J. Huang and S. W. Lee, "Tri-band frequency selective surface with circular ring elements," in *Antennas and Propagation Society International Symposium*, pp. 204-207, 1991.

[12] R. Janaswami and D. H. Schaubert, "Characteristic impedance of a wide slot line on low permittivity substrates," *IEEE Trans. Microw. Theory Techn.*, vol. 34, no. 8, pp. 900-902, 1986.

[13] D. Hotte, R. Siragusa, Y. Duroc, and S. Tedjini, "Radar cross-section measurement in millimetre-wave for passive millimetre-wave identification tags," *IET Microw. Antennas Propag.*, vol. 9, pp. 1-7, 2015.

[14] A. Vena, E. Perret, and S. Tedjni, "A depolarizing chipless RFID tag for robust detection and its FCC compliant UWB reading system," *IEEE Trans. Microw. Theory Techn.*, vol. 61, no. 8, pp. 2982-2994, 2013.

[15] M. I. Skolnik, *Radar Handbook.* New York: McGraw-Hill, 1970.

[16] A. Vena, E. Perret, and S. Tedjini, "A fully printable chipless RFID tag with detuning correction technique," *IEEE Microw. Wireless Compon. Lett.*, vol. 22, no. 4, pp. 209-211, 2012.

[17] M. A. S. Miacci, E. L. Nohara, I. M. Martin, *et al.*, "Indoor radar cross section measurements of simple targets," *J. Aerosp. Technol. Manag.*, vol. 4, pp. 25-32, 2012.